

Zero-Degree Fragmentation of Relativistic ${}^6\text{Li}$

C. L. Ruiz, R. W. Huggett, and P. N. Kirk

Department of Physics and Astronomy, Louisiana State University, Baton Rouge, Louisiana 70803

(Received 6 March 1979)

Evidence for the dissociation of relativistic ${}^6\text{Li}$ ions into the channels ${}^3\text{H} + {}^2\text{H} + p$ and ${}^3\text{He} + {}^2\text{H} + n$ is presented. The number of events in each of these secondary channels is approximately 20% of the number of events in the channel ${}^6\text{Li} \rightarrow {}^4\text{He} + {}^2\text{H}$. Possible mechanisms for populating the secondary channels are discussed.

The nucleus ${}^6\text{Li}$ is often discussed in theories of cluster structure.¹⁻³ Because it is bound by only 1.47 MeV against dissociation into ${}^4\text{He}$ and ${}^2\text{H}$, the ground state of ${}^6\text{Li}$ is expected to exhibit strong ${}^4\text{He}$ - ${}^2\text{H}$ clustering.⁴⁻⁶ Within the context of present theories and the impulse approximation the ${}^4\text{He}$ - ${}^2\text{H}$ final state is expected to be an important channel in the dissociation of ${}^6\text{Li}$,⁷ and this expectation has been confirmed experimentally in low-energy cluster-knockout reactions.⁸⁻¹⁰

In this paper we present the first results from an experiment designed to detect in coincidence two charged ions produced in the dissociation of relativistic ${}^6\text{Li}$. The primary dissociation channel in this experiment was observed to be ${}^6\text{Li} \rightarrow {}^4\text{He} + {}^2\text{H}$, and we shall report on the characteristics of this channel later. The purpose of this paper is to report the observation of unexpected signals produced in secondary dissociation channels of ${}^6\text{Li}$ and to suggest mechanisms for their production. The secondary dissociation channels are ${}^6\text{Li} \rightarrow {}^3\text{He} + {}^2\text{H} + (n)$ and ${}^6\text{Li} \rightarrow {}^3\text{H} + {}^2\text{H} + (p)$, where the parentheses enclose unobserved ions. These signals were unexpected because these channels have neither the theoretical foundation of the ${}^4\text{He}$ - ${}^2\text{H}$ channel nor a history of repeated observations.

The data were taken at the Bevalac in one of the 0° beam lines, a schematic of which is shown

in Fig. 1. The projectiles were fully stripped ${}^6\text{Li}$ ions with total kinetic energy 11.8 GeV. The presence of a projectile was established by a triple coincidence between scintillation counters T1, T2, and T3. The target for this experiment was ${}^{12}\text{C}$ of thickness 6 g cm^{-2} . Projectiles that passed through the target without dissociating were identified and rejected in the electronics by means of pulse heights in the scintillation counter labeled ANTI in Fig. 1. The identification of unfragmented ${}^6\text{Li}$ ions was straightforward because dE/dx is proportional to the square of the charge, and pulse heights produced by triply charged ions were well separated from those produced by coincident pairs of singly and doubly charged ions. The experiment contained two hodoscopes, an eight-element array, labeled G, at the entrance to the vacuum tank, and a thirty-element array, labeled R, at the rear of the counting area. The integrated B/l through the bending magnets was measured by wire orbiting for charge-to-mass (Z/A) ratios of $\frac{1}{3}$, $\frac{1}{2}$, and $\frac{2}{3}$. The value of B/l for ions with a Z/A ratio of $\frac{1}{2}$ was 40.26 kG m. The interiors of the magnets and the drift spaces were enclosed in vacuum tanks to suppress secondary fragmentation. The objects labeled SC1-SC10 were multiwire spark chambers with magnetostrictive readout. Surrounding the target on four sides was a counter,

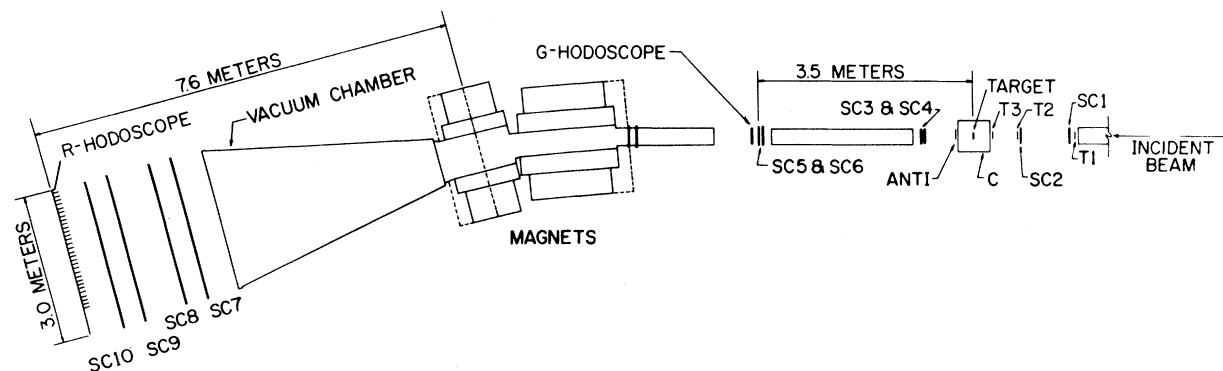


FIG. 1. Schematic of beam line 38 at the Bevalac.

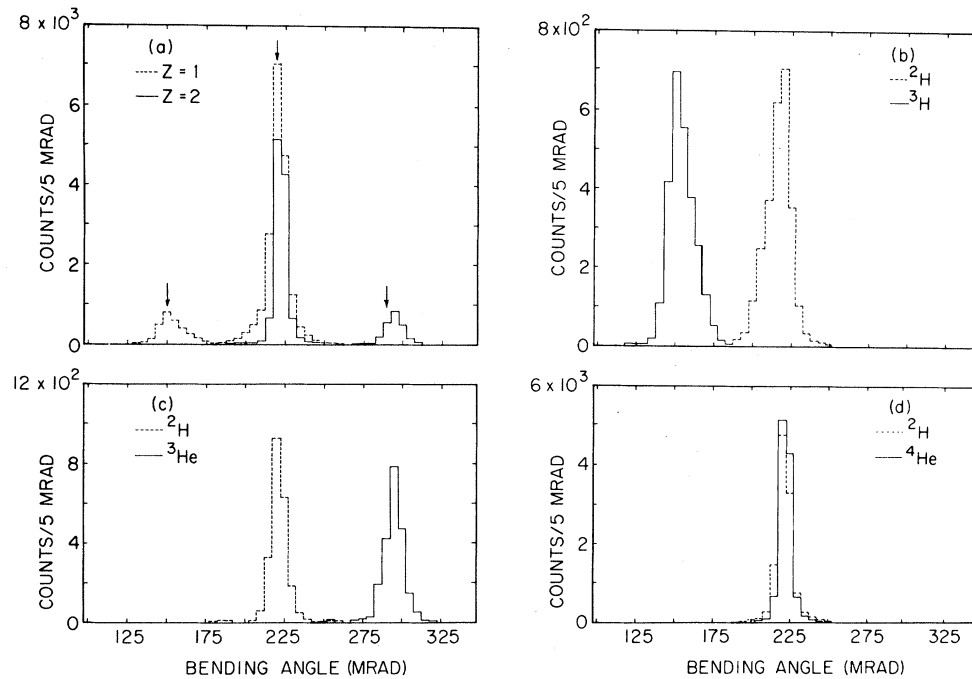


FIG. 2. Histograms of events versus bending angle. (a) Master histogram comprising all events. (b) Events in ${}^2\text{H}$ - ${}^3\text{H}$ coincidence channel. (c) Events in ${}^2\text{H}$ - ${}^3\text{He}$ coincidence channel. (d) Events in ${}^2\text{H}$ - ${}^4\text{He}$ coincidence channel.

labeled C in Fig. 1, that contained alternate layers of lead and scintillator. The purpose of the C counter was to identify those interactions accompanied by meson production, particle emission at wide angles, or by excitation of the target nucleus.

The normal electronic logic for establishing the existence of an event was $\text{T1} \cdot \text{T2} \cdot \text{T3} \cdot \overline{\text{ANTI}} \cdot \overline{\text{C}} \cdot \text{G}(2) \cdot \text{R}(2)$, where the symbols G(2) and R(2) represent the requirement of signals from any two members of the respective hodoscopes.

The nominal acceptance of the spectrometer was ± 13 mrad in the horizontal plane and ± 9 mrad in the vertical plane.

Charges were measured by means of their pulse heights in scintillator, and typical spectra accumulated in this experiment have been presented elsewhere.¹¹

In Fig. 2(a) is displayed a histogram of events versus bending angle. These data were produced by 8.189×10^6 incident ${}^6\text{Li}$ projectiles. The background subtraction amounted to 8% and was due primarily to fragmentation in T3.

The arrows denote predicted deflection angles for ions with Z/A ratios of $\frac{1}{3}$, $\frac{1}{2}$, and $\frac{2}{3}$. These angles were calculated from the formula $\theta = (3.218 \times 10^{-2} \text{ kG}^{-1} \text{ m}^{-1}) (Z/A)(Bl/\beta\gamma)$, where $\beta\gamma$ is calculated from the known velocity of the projec-

tiles. The approximate equality between the velocities of the fragments and the projectiles is one of the distinctive and simplifying characteristics of 0° fragmentation. It was established experimentally in one of the early experiments of Heckman *et al.*¹² In addition, this experiment is directly sensitive to the velocities of the fragments, and a broad distribution of velocities would degrade the mass resolution exhibited in Fig. 2.

We attribute the peak at 150 mrad to ${}^3\text{H}$ ions, the large central peak at 220 mrad to a mixture of ${}^2\text{H}$ and ${}^4\text{He}$ ions, and the peak at 295 mrad to ${}^3\text{He}$ ions. The decomposition of the raw spectrum into coincidence channels is presented in Figs. 2(b), 2(c), and 2(d). Figure 2(b) shows that the ${}^3\text{H}$ ions are in coincidence with ${}^2\text{H}$ ions. From Fig. 2(c) one sees that the ${}^3\text{He}$ ions are also in coincidence with ${}^2\text{H}$ ions. Figure 2(d) shows that the central peak is largely due to coincidences between ${}^2\text{H}$ and ${}^4\text{He}$, as expected. The total numbers of coincidences represented in Figs. 2(a), 2(b), 2(c), and 2(d) are 18 582, 2775, 2418, and 11 851, respectively. The sum of the numbers of events in Figs. 2(b), 2(c), and 2(d) does not equal the number of events in 2(a) because of coincidences attributable to other dissociation channels.

The central points of this paper are, first, that we have observed unexpected secondary dissociation channels of ${}^6\text{Li}$ and, second, that under the conditions of this experiment these secondary channels appear with a strength of approximately 0.2 times the strength of the principal signal.

Of the mechanisms that might be proposed to account for these signals the simplest is secondary fragmentation of the α particles. We have rejected this hypothesis for several reasons but primarily because it is inconsistent with direct measurement. An Al absorber of thickness 5.14 g cm^{-2} was inserted into the beam line immediately behind the G hodoscope. Assuming the validity of this hypothesis, one can readily calculate the changes in the percentages of events in the principal and secondary channels, and these changes were not observed.

The nucleus ${}^6\text{Li}$ has broad excited states at 25 and 26.6 MeV which lie 3–5 MeV above the threshold for dissociation into ${}^3\text{He} + {}^2\text{H} + n$ and ${}^3\text{H} + {}^2\text{H} + p$. One possible production mechanism for the secondary signals observed in this experiment is direct excitation of the ${}^6\text{Li}$ nucleus into one of these states followed by the free decay of the excited state. However, these ${}^6\text{Li}^*$ levels also lie above the threshold for decay into ${}^3\text{He} + {}^3\text{H}$. We have calculated the efficiency for detecting in our apparatus both final-state ions in the decay ${}^6\text{Li}^* \rightarrow {}^3\text{He} + {}^3\text{H}$ and have concluded that this hypothesis is not tenable unless the ${}^6\text{Li}^*$ excited states are assumed to decay almost exclusively through the channels ${}^3\text{He} + {}^2\text{H} + n$ and ${}^3\text{H} + {}^2\text{H} + p$.

Although the unexpected signals could be produced by the direct coupling of the ${}^6\text{Li}$ ground state to the secondary channels, this hypothesis cannot be sustained on the basis of the data presented here. The hypothesis could be tested directly in low-energy cluster-knockout experiments such as ${}^6\text{Li}(p, p^3\text{He}){}^2\text{H}n$.

In addition to direct coupling there are couplings through excited states of ${}^4\text{He}$, ${}^5\text{He}$, and ${}^5\text{Li}$ which could account for the secondary signals observed in this experiment. The Feynman diagrams for these sequential processes are illustrated in Fig. 3(a) for four decays of interest: (1) $A = {}^4\text{He}^*$, $B = {}^2\text{H}$, $C = {}^3\text{He}$, $D = n$; (2) $A = {}^4\text{He}^*$, $B = {}^2\text{H}$, $C = {}^3\text{H}$, $D = p$; (3) $A = {}^5\text{Li}^*(16.7)$, $B = n$, $C = {}^2\text{H}$, $D = {}^3\text{He}$; (4) $A = {}^5\text{He}^*(16.7)$, $B = p$, $C = {}^2\text{H}$, $D = {}^3\text{H}$.

The ${}^4\text{He}$ nucleus has three excited states between 20.1 and 22.1 MeV that are known to decay into the secondary channels observed in this experiment. However, the 20.1-MeV level decays solely through the ${}^3\text{H} + p$ channel, which makes

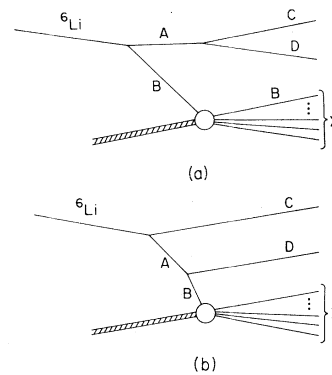


FIG. 3. Feynman diagrams illustrating production mechanisms for signals in secondary channels through (a) sequential processes and (b) single-nucleon emission by virtual nuclei.

it difficult to reconcile this hypothesis with the approximate equality between the numbers of events in the two secondary channels. In addition, this hypothesis does not appear to be consistent with low-energy experiments. The most pertinent data to date have been provided by MacKenzie and Mark,¹³ who carried out an experiment on the reaction ${}^6\text{Li}(p, pd){}^4\text{He}$ at 100 MeV. They found that the strength of the transition to the 20-MeV excited states of ${}^4\text{He}$ is only about 10% of the strength of the transition to the ground state.

The nucleus ${}^5\text{He}$ has a $\frac{3}{2}^+$ excited state at an energy of 16.76 MeV. This state lies 60 keV above the threshold for dissociation into ${}^2\text{H} + {}^3\text{H}$ and is often regarded as an S-state resonance of ${}^2\text{H}$ and ${}^3\text{H}$. The isobaric analog state in ${}^5\text{Li}$ lies 16.66 MeV above the ground state and 270 keV above the threshold for disintegration into ${}^3\text{He}$ and ${}^2\text{H}$. The secondary signals could be readily understood if the wave function for the ${}^6\text{Li}$ ground state were to contain sizable components of the ${}^5\text{He}^*(16.8)-p$ and ${}^5\text{Li}^*(16.7)-n$ configurations. It is known that removing a proton from the S shell of ${}^6\text{Li}$ produces the 16.8-MeV excited level of ${}^5\text{He}$ and that removing a neutron from the S shell produces the 16.7-MeV level of ${}^5\text{Li}$.¹⁴⁻¹⁸ Thus, there is an experimentally demonstrated mechanism for producing these excited states. There is also some theoretical support for this hypothesis. Schutte *et al.*¹⁹ have suggested that the ${}^4\text{He}-{}^2\text{H}$ scattering system is coupled to both configurations and that virtual transitions through these configurations may play some role in understanding the reaction ${}^4\text{He} + {}^2\text{H} \rightarrow {}^3\text{H} + {}^3\text{He}$ at low energies.

Lukyanov and Titov,²⁰ and also Glagolav *et al.*,²¹ have suggested that nucleon transfer may be one of the mechanisms by which nuclei dissociate, and this hypothesis does provide a convenient means for producing the secondary signals observed in this experiment. The Feynman diagrams in Fig. 3(b) illustrate the mechanism for four cases of interest: (1) $A=^3\text{H}$, $B=n$, $C=^3\text{He}$, $D=^2\text{H}$; (2) $A=^3\text{He}$, $B=p$, $C=^3\text{H}$, $D=^2\text{H}$; (3) $A=^4\text{He}$, $B=p$, $C=^2\text{H}$, $D=^3\text{H}$; (4) $A=^4\text{He}$, $B=n$, $C=^2\text{H}$, $D=^3\text{He}$.

Nucleon transfer reactions are well established in low-energy nuclear physics, and their role in mediating the interactions between nuclei at intermediate energies needs attention. In comparison with the mass of the pion, nuclei are loosely bound against dissociation into a nucleon and another nucleus. Using the original ideas of Good and Walker,²² one concludes that the range of nucleon transfer reactions might exceed the range of interactions involving pion exchange.

Of the production mechanisms discussed in the preceding paragraphs the two most promising, in our opinion, are sequential decay through the 16.7-MeV excited states of ^5Li and ^5He and single-nucleon emission by virtual nuclei. A useful next step would be to determine which of these mechanisms, if indeed either, can be justified theoretically.

This research was supported by U. S. Department of Energy Contract No. EY-76-S-05-4699.

- ¹Mamta Rai *et al.*, Phys. Lett. **59B**, 327 (1975).
- ²B. Mithra and R. Laverriere, Phys. Lett. **58B**, 17 (1975).
- ³Y. Sakamoto *et al.*, Phys. Rev. C **11**, 668 (1975).
- ⁴T. K. Lim, Phys. Lett. **56B**, 321 (1975).
- ⁵J. V. Noble, Phys. Lett. **55B**, 433 (1975).
- ⁶G. R. Plattner *et al.*, Phys. Lett. **61B**, 21 (1976).
- ⁷D. Miljanic *et al.*, Phys. Lett. **50B**, 330 (1974).
- ⁸G. Landaud *et al.*, Phys. Rev. C **18**, 1776 (1978).
- ⁹P. G. Roos *et al.*, Phys. Rev. C **15**, 69 (1977).
- ¹⁰P. G. Roos *et al.*, Nucl. Phys. **A257**, 317 (1976).
- ¹¹C. L. Ruiz *et al.*, Nucl. Instrum. Methods **159**, 55 (1979).
- ¹²H. H. Heckman *et al.*, Phys. Rev. Lett. **28**, 926 (1972).
- ¹³I. A. MacKenzie and S. K. Mark, Nucl. Phys. **A178**, 225 (1971).
- ¹⁴Yu. P. Antoufiev *et al.*, Phys. Lett. **42B**, 347 (1972).
- ¹⁵Ranjan K. Bhowmik *et al.*, Nucl. Phys. **A226**, 365 (1974).
- ¹⁶S. N. Gardiner *et al.*, Phys. Lett. **46B**, 186 (1973).
- ¹⁷L. A. Kull, Phys. Rev. **163**, 1066 (1967).
- ¹⁸D. Bachelier *et al.*, Nucl. Phys. **A126**, 60 (1969).
- ¹⁹W. Schutte *et al.*, Phys. Lett. **65B**, 214 (1976).
- ²⁰V. K. Lukyanov and A. I. Titov, Phys. Lett. **57B**, 10 (1975).
- ²¹V. V. Glagolev *et al.*, Phys. Rev. C **18**, 1382 (1978).
- ²²M. L. Good and W. D. Walker, Phys. Rev. **120**, 1855, 1857 (1960).

Test of the Interacting-Boson-Approximation Model for Odd-Mass Nuclei

R. F. Casten and G. J. Smith

Brookhaven National Laboratory, Upton, New York 11973

(Received 11 April 1979)

The interacting-boson-approximation model has recently been extended to odd- A nuclei. The first extensive test of the new model gives good agreement for unique-parity levels in ^{109}Pd , where the particle-rotor model cannot reproduce empirical results.

The interacting-boson-approximation (IBA) model^{1,2} of Arima, Iachello, and co-workers has evoked considerable interest because it offers a unified treatment of the collective states of all heavy even-even nuclei except those at or adjacent to closed shells. It has recently had considerable success,^{3,4} and has led directly to the prediction and subsequent discovery³ of a new nuclear symmetry, the O(6) limit. However, its application to odd-mass nuclei has been limited⁵ to a few qualitative arguments and limiting situations. Very recently, though, the recognition^{6,7} of the importance of an exchange term in the bos-

on-fermion interaction has allowed the development of a general model (interacting boson-fermion approximation or IBFA) which includes a rich variety of level sequences reminiscent of widely different geometrical coupling schemes and of empirical odd-mass nuclei.

The favored high-spin, negative-parity levels in the odd-mass Pd isotopes (e.g., ^{105}Pd) have been interpreted⁸ as $h_{11/2}$ rotation-aligned⁹ (decoupled) bands with spin sequences $\frac{11}{2} \pm 2n$ where $n = 0, 1, 2, \dots$. These unique-parity states thus belong to an isolated family since the other low-lying levels originate in the positive-parity orbits